

See discussions, stats, and author profiles for this publication at: <https://www.researchgate.net/publication/258037631>

# Copper(II) Complexes with 4-Carbomethoxypyrrolidone Functionalized PAMAM-Dendrimers: an EPR Study.

ARTICLE in THE JOURNAL OF PHYSICAL CHEMISTRY B · OCTOBER 2013

Impact Factor: 3.3 · DOI: 10.1021/jp410307z · Source: PubMed

---

CITATIONS

7

READS

73

## 8 AUTHORS, INCLUDING:



Maria Francesca Ottaviani

Università degli Studi di Urbino "Carlo Bo"

88 PUBLICATIONS 2,011 CITATIONS

[SEE PROFILE](#)



Michela Cangiotti

Università degli Studi di Urbino "Carlo Bo"

45 PUBLICATIONS 336 CITATIONS

[SEE PROFILE](#)



Alberto Fattori

Università degli Studi di Urbino "Carlo Bo"

12 PUBLICATIONS 95 CITATIONS

[SEE PROFILE](#)



Jørn B. Christensen

University of Copenhagen

140 PUBLICATIONS 1,983 CITATIONS

[SEE PROFILE](#)

# Copper(II) Complexes with 4-Carbomethoxypyrrolidone Functionalized PAMAM-Dendrimers: An EPR Study

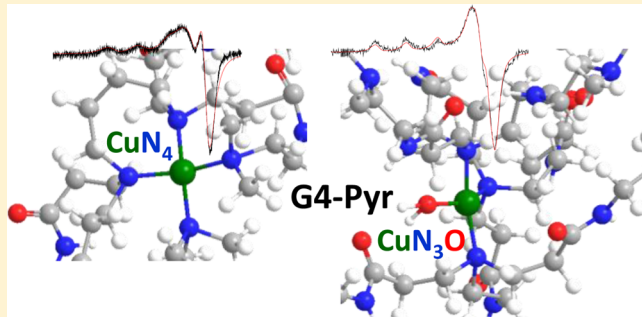
Maria Francesca Ottaviani,<sup>\*,†</sup> Michela Cangiotti,<sup>†</sup> Alberto Fattori,<sup>†</sup> Concetta Coppola,<sup>†</sup> Susanna Lucchi,<sup>†</sup> Mario Ficker,<sup>‡</sup> Johannes F. Petersen,<sup>‡</sup> and Jørn B. Christensen<sup>\*,‡</sup>

<sup>†</sup>Department of Earth, Life and Environment Sciences, University of Urbino, Località Crocicchia, 61029 Urbino, Italy

<sup>‡</sup>Department of Chemistry, University of Copenhagen, Universitetsparken 5, DK-2100, Copenhagen, Denmark

## Supporting Information

**ABSTRACT:** The internal flexibility and interacting ability of PAMAM-dendrimers having 4-carbamethoxypyrrolidone-groups as surface groups (termed Gn-Pyr), which may be useful for biomedical purposes, and ion traps were investigated by analyzing the EPR spectra of their copper(II) complexes. Increasing amounts (with respect to the Pyr groups) of copper(II) gave rise to different signals constituting the EPR spectra at room and low temperature corresponding to different coordinations of Cu<sup>2+</sup> inside and outside the dendrimers. At low Cu<sup>2+</sup> concentrations, CuN<sub>4</sub> coordination involving the DAB core is preferential for G3- and G5-Pyr, while G4-Pyr shows a CuN<sub>3</sub>O coordination. CuN<sub>2</sub>O<sub>2</sub> coordination into the external dendrimer layer was also contributing to G3- and G4-Pyr spectra. The structures of the proposed copper–dendrimer complexes were also shown. G4-Pyr displays unusual binding ability toward Cu(II) ions. Mainly the remarkably low toxicity shown by G4-Pyr and its peculiar binding ability leads to a potential use in biomedical fields.



## INTRODUCTION

Dendrimers are well-defined synthetic macromolecules built by repetitive branching from a core, which can be viewed as a nanomodule in the nanoperiodic table.<sup>1,2</sup> Dendrimers are characterized by having a large number of external surface groups controlling most of the physical properties. These may also be differently functionalized with biomolecular relevant moieties. The dendrimer interior, depending on the actual branch cell and the number of generations (Gn), can have cavities capable of hosting small molecules or ions. Therefore, dendrimers may work as drug carriers and ion traps.<sup>3–5</sup> Nanomedicine is one of the research areas where dendrimers play an important role, because they offer a high degree of structural control and diversity.<sup>3–5</sup> We recently found that a G4 PAMAM-dendrimer having 64 4-carbamethoxypyrrolidone-groups as surface groups (indicated as G4-Pyr) shows unusually low toxicity in a series of in vitro cell assays, including very weak interactions with proteins.<sup>6,7</sup> Because this low toxicity could lead to applications as a new guest–host drug-delivery platform, it is of interest to investigate the internal structure of these compounds and their interacting ability. In this respect, the electron paramagnetic resonance (EPR) technique has been found to be very useful to characterize the dendrimer interacting ability by using copper(II) ions as probes<sup>8–16</sup> and nitroxide radicals to study dendrimer interactions in solution with biomolecules and biostructures.<sup>12–21</sup> In these previous studies it was verified that Cu(II) complexation is particularly informative about the internal structure of the dendrimers in

solution and to differentiate the internal/external interacting sites in respect to their availability for ion trapping. In this study, we performed an EPR analysis of copper(II) complexes with Gn-Pyr dendrimers at different generations (G3–5) having the following chemical formulas (the structure of G4-Pyr is illustrated in Figure 1):



dendri PAMAM(PYR-COO<sub>Me</sub>)<sub>32</sub>: termed G3-Pyr



dendri PAMAM(PYR-COO<sub>Me</sub>)<sub>64</sub>: termed G4-Pyr



dendri PAMAM(PYR-COO<sub>Me</sub>)<sub>128</sub>: termed G5-Pyr

Cu<sup>2+</sup> ions were used as probes to study the structure and interacting ability of the Gn-Pyr dendrimers by changing the relative concentration of these ions with respect to the external dendrimer functionality (the pyrrolidone units). Spectra at both room and low temperature were compared to obtain information on the investigated system.

Received: October 17, 2013

Revised: October 23, 2013

Published: October 23, 2013



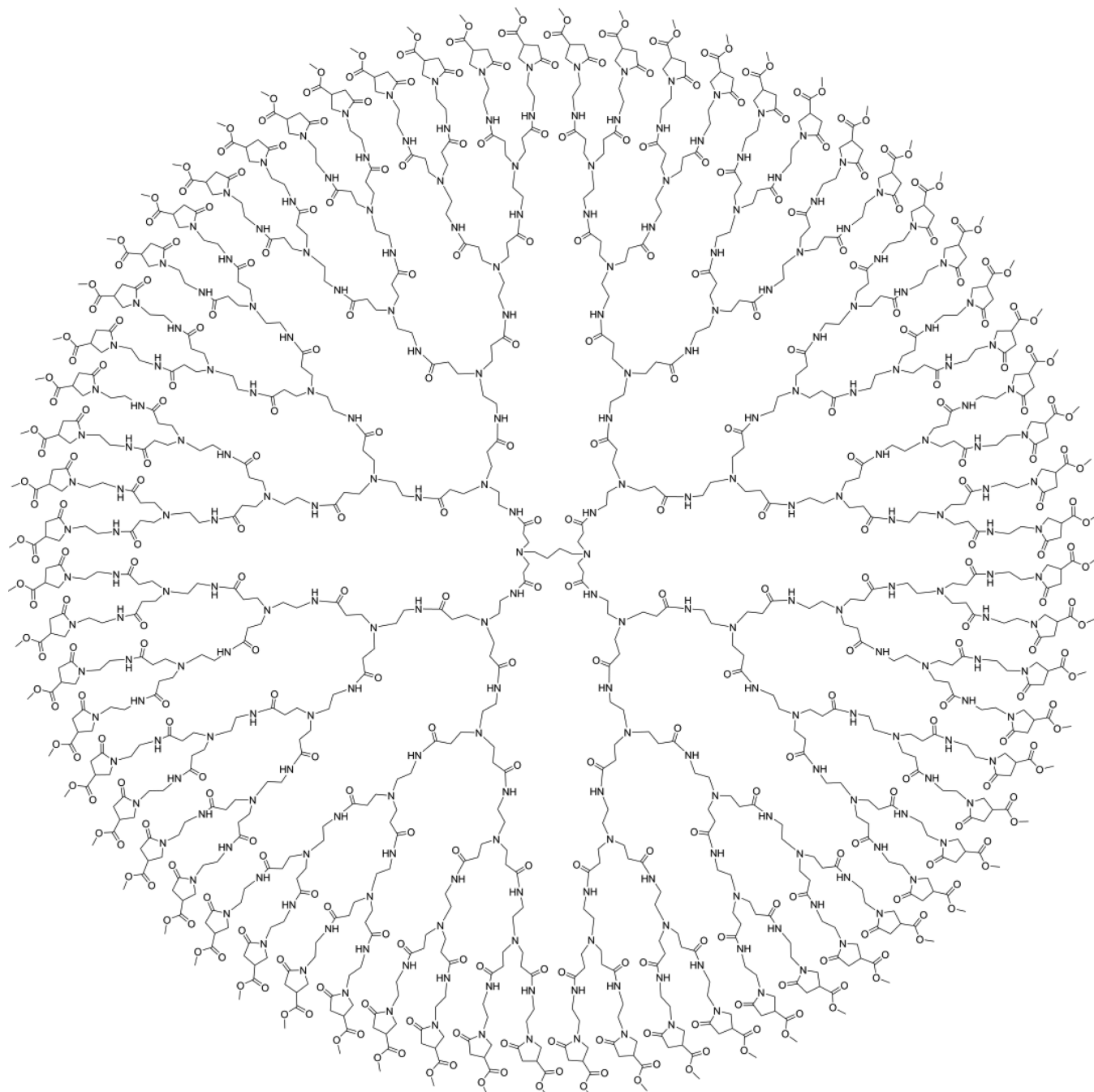


**Figure 1.** Structure of the DAB-cored G4 PAMAM-dendrimer with 64 4-carbomethoxypyrrolidone-groups.

## ■ EXPERIMENTAL SECTION

**Materials and Sample Preparation.** The dendrimers were synthesized according to published procedures.<sup>22</sup> The dendrimers were subsequently functionalized with 4-carbomethoxy pyrrolidone groups.<sup>46</sup> The dendrimers were dissolved in Millipore doubly distilled water resulting in a final surface group concentration of 0.1 M. Cupric nitrate hydrate ( $\text{Cu}(\text{NO}_3)_2 \cdot 2.5\text{H}_2\text{O}$ , Sigma-Aldrich, ACS reagent 98%) was also dissolved in Millipore doubly distilled water to obtain a final concentration, in the mixture with the dendrimers, from 0.0025 to 0.5 M. After different equilibration times (from freshly prepared to one day aging), 100  $\mu\text{L}$  of the dendrimer-copper solution was inserted in an EPR tube (1 mm internal diameter).

**Methods.** EPR spectra were recorded by means of an EMX-Bruker spectrometer operating at X band (9.5 GHz) and interfaced with a PC (software from Bruker for handling and analysis of the EPR spectra). The temperature was controlled with a Bruker ST3000 variable-temperature assembly cooled with liquid nitrogen. The EPR spectra were recorded for the different samples at 298 K and 150 K.

In all cases, we controlled the reproducibility of the results by repeating the EPR analysis (three times) in the same experimental conditions for each sample.

**Simulation of the EPR Spectra and Identification of Cu(II)-Coordination Sites and Structures.** The low temperature EPR spectra were computed by using (and comparing) different methods: (a) the CU23 program kindly provided by

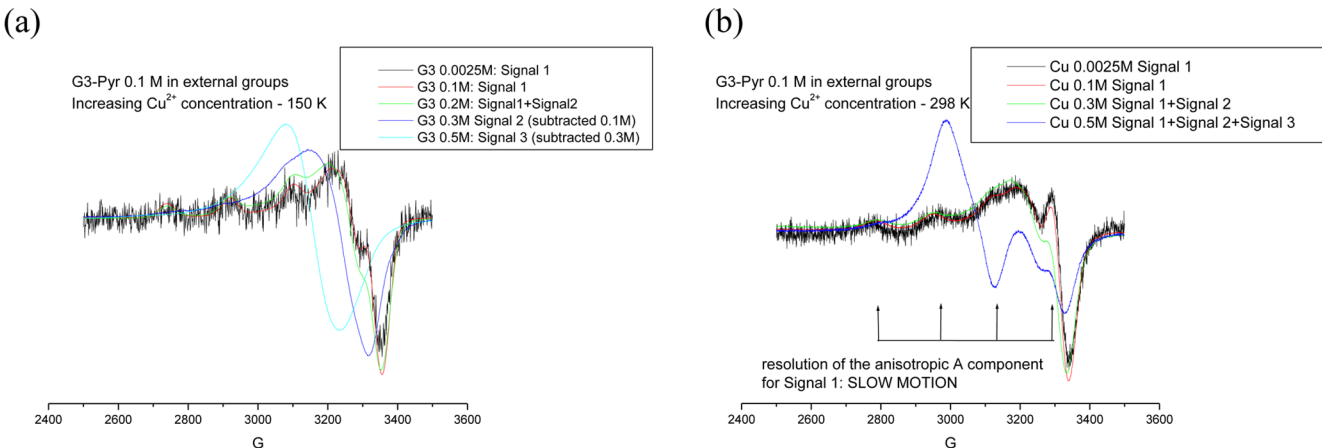


**Figure 2.** Selected EPR experimental spectra of G3-pyr (0.1 M in surface groups, corresponding to about 0.003 M in dendrimer macromolecules) at 150 K (a) and 298 K (b) at different Cu(II) concentrations, normalized at the same heights.

Prof. Romanelli, University of Florence, Italy; (b) the Bruker's WIN-EPR SimFonia Software Version 1.25; (c) the method reported by Bennett et al.;<sup>23,24</sup> (d) the program EasySpin 4.5.1, using MATLAB 7.5; (e) the procedure by Budil et al. for computing nitroxide radical spectra,<sup>25</sup> which may be successfully applied to the simulation of Cu(II) spectra, too. This last program was also used to compute the spectra at 298 K, thus, providing information about the mobility of the Cu complex (the correlation time for the diffusion rotational motion of the complexed Cu(II) ions,  $\tau$ ), which is related to the flexibility of the dendrimer structure in the region where Cu<sup>2+</sup> is located. We considered satisfactory a simulation that produces the best fitting between the experimental and the simulated spectra. By comparing the different simulation procedures, we found that the most satisfactory and also providing the most information about our systems was Budil and Freed program, which allowed us to verify the magnetic parameters in computing the spectra at both room and low temperature. Therefore, in Results and Discussion, we mainly show the results obtained by using this procedure. The main magnetic parameters used for the simulation of the spectra at both low and room temperatures were (a) the  $g_{ii}$  components (accuracy in the third decimal, on the basis of the simulation itself) for the coupling between the electron spin and the magnetic field; (b) the  $A_{ii}$  components (accuracy of about 3%) for the coupling between the electron spin and the nuclear spin ( $I_{\text{Cu}} = 3/2$ ); and (c) the line widths  $W_i$  of the  $x$ ,  $y$ , and  $z$  lines (accuracy about 3%). The magnetic parameters were first directly measured in the spectra by field calibration with the DPPH radical ( $g = 2.0036$ ), and then we used these parameters as starting values for the spectra simulation, changing them until the best fitting between the experimental and the simulated spectra was obtained.

In several cases, the spectra were constituted by two or three components due to different coordination and geometries of Cu(II)-dendrimer complexes. The subtraction between the spectra in different experimental conditions allowed extraction of the spectral components constituting the overall EPR spectra. The different components were computed separately. The subtraction procedure also allowed us to calculate, by double integration of each component, the relative percentages of the different components, with an accuracy of 3%.

We found that the simulations of the observed EPR signals provided a useful means of estimating the spectral parameters but did not necessarily produce unique fits. However, we

trusted the parameters which provided best fitting of a series of spectra in similar experimental conditions.

The magnetic parameters extracted from the simulation were then compared with equivalent parameters found in the literature.<sup>8–11,26–44</sup> This allowed us to assign each spectral component to a copper coordination and identify the structure and complexing sites of the dendrimers.

Because we also wanted to compare the spectral intensities (obtained by double integration of the spectra) to verify if strong spin–spin interactions decrease the intensity itself, the spectra were all recorded in the same experimental conditions, that is, the same receiver gain ( $6.32 \times 10^2$ ), modulation amplitude (3 G), time constant (10.24 ms), conversion time (40.96 ms), resolution (2048 points), number of scans (10 scans), EPR tube size (1 mm internal), liquid volume (50  $\mu\text{L}$ ), temperature (298 and 150 K), position inside the EPR cavity, and of course, controlling the reproducibility of the spectra for repeated preparations of the same sample also for their intensities. The reverse of the medal in such procedure is that the spectra at the lowest copper(II) concentrations were very noisy, but we trusted the procedure if the magnetic components were recognizable and we could perform their simulations.

## RESULTS AND DISCUSSION

The EPR results are discussed in the following, starting from G3-Pyr. However, after G3-Pyr, we will describe and compare the EPR results obtained from G5-Pyr, instead of following the apparently more logical sequence to discuss G4-Pyr results, after G3 and before G5. The reason for this choice is that G3- and G5-Pyr behave in a similar way, while G4-Pyr shows a different behavior when titrated with increasing Cu(II) concentrations.

Figure 2 shows some selected experimental EPR spectra and subtracted signals of G3-Pyr (0.1 M in surface groups, corresponding to about 0.003 M in dendrimer macromolecules) at 150 K (Figure 1a) and 298 K (Figure 1b) with different Cu<sup>2+</sup> concentrations, normalized at the same heights. The spectra were superimposed to better point out the spectral variations as a function of copper(II) concentration.

It can be seen that the spectra are not changing in the Cu(II) concentration range from 0.0025 to 0.1 M. The simulations of this signal, termed Signal 1, are shown in Figure S1a (150 K) and Figure S1b (298 K) in the Supporting Information, for a

**Table 1. Magnetic and Mobility Parameters (Accuracy 2%) Extracted from the Simulations of the EPR Signals for Gn-Pyr Dendrimers (0.1 M in Surface External Groups) with Cu<sup>2+</sup> Concentrations Selected as Representative of the System Behavior (Simulations Shown in the Supporting Information)**

signal	Gn	%	[Cu <sup>2+</sup> ]	g <sub>xx</sub>	g <sub>yy</sub>	g <sub>zz</sub>	A <sub>xx</sub> (G)	A <sub>yy</sub> (G)	A <sub>zz</sub> (G)	τ <sup>a</sup> (ns)	LW <sup>b</sup> (G)
water	no	100	0.0025–0.5	2.100	2.100	2.450	10	10	115	0.05	50 <sup>c</sup>
1	G3	100	0.0025–0.1	2.055	2.100	2.268	5	20	181	1.67	25
	G4	55	0.05								
	G5	55	0.025								
1	G4	50	0.025	2.055	2.100	2.268	5	20	181	5.3	15
1	G5	72	0.01	2.055	2.100	2.268	20	20	180	1.67	10
2	G3	38	0.3	2.080	2.130	2.290	25	25	150	15	50
	G4	35	0.3								
	G5	28	0.01								
	G3	30	0.5	2.090	2.090	2.350	5	5	125	0.3	40 <sup>c</sup>
	G4	75	0.5								
3	G5	88	0.3								
	G4	100	0.005	2.070	2.100	2.320	15	10	160	0.8	25
4	G4	50	0.025	2.070	2.100	2.320	15	10	160	0.3	25

<sup>a</sup>At 298 K. <sup>b</sup>Line width. <sup>c</sup>Simulation needed a Heisenberg exchange frequency  $W_{\text{ex}} = 1.6 \times 10^8 \text{ s}^{-1}$ .

Cu(II) concentration of 0.01 M. The magnetic parameters used for the simulations are listed in Table 1.

Similar magnetic parameters were found for the EDA-core amino terminated PAMAM-dendrimers at similar copper/dendrimer concentrations.<sup>8–11</sup> These parameters indicated a square planar (partially distorted) Cu–N<sub>4</sub> coordination which may only occur for Cu(II) ions trapped internally in the dendrimer. A bigger difference between the *x* and *y* components was found for the pyrrolidone dendrimer with respect to the amino-terminated dendrimer, which indicates a more distorted (anisotropic) coordination structure. The coordination mode proposed by Diallo et al.<sup>45</sup> involving the tertiary nitrogen sites of the first generation layer is the most probable. In alternative, we propose a CuN<sub>4</sub> structure where the Cu(II) ions coordinate with the nitrogen sites of the DAB core and two other tertiary amines in the close branches (Figure 3a).

The structure proposed in Figure 3a is mainly based on the simulation of the spectrum at 298 K (Figure S1b, Supporting Information), which indicates a mobility of the ions ( $\tau = 1.67$  ns, Table 1) at the limit of the so-called “slow motion” conditions ( $10 \text{ ns} > \tau > 1\text{--}2 \text{ ns}$ ). Such a slow mobility is well justified by Cu(II) binding the dendrimer core which has low degrees of freedom. The results from G5-Pyr will also support this finding.

By increasing the copper concentration above 0.1 M, the line shape progressively changes (Figure 1a,b). First, we noted (results not shown) that the spectral intensity (obtained by double integration of the spectra) almost linearly increases with Cu(II) concentration. This evidence excludes the occurrence of strong spin–spin interactions or dimeric Cu(II) complexes which usually impede the ability to record EPR spectra at room temperature. The subtraction of Signal 1 from the spectra at Cu(II) concentrations over 0.1 M leads to the extraction of a second signal termed Signal 2, which was computed as shown in Figure S1c (Supporting Information). Its line shape poorly changes from 150 to 298 K, indicating very slow mobility conditions even at room temperature. The simulation parameters for Signal 2 reported in Table 1 suggest, by comparison with literature parameters,<sup>8–11,26–37</sup> a CuN<sub>2</sub>O<sub>2</sub> distorted square planar coordination. The very slow motion conditions at room temperature and the invariance over

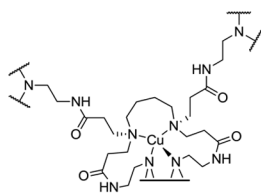
temperature indicate that the copper ions are inside the dendrimer, close to the external surface, in the most crowded dendrimer region where the branches approach each other. The location just below the surface groups indicates that the oxygen sites of CuN<sub>2</sub>O<sub>2</sub> are close to nitrogen atoms as in the amido or pyrrolidone groups. The line broadening is probably caused by oxygen generating weak spin–spin interactions with the ions. Figure 3b sketches the proposed CuN<sub>2</sub>O<sub>2</sub> coordination inside the dendrimer.

At copper concentrations  $\geq 0.3$  M, a third signal (termed Signal 3) starts contributing to the EPR spectrum (Figure 1a,b). Its simulation is shown in Figure S1d (Supporting Information), while the main parameters used for the simulations are listed in Table 1. These simulation parameters are characteristic of a CuO<sub>4</sub> coordination, which arises from copper ions outside the dendrimers and interacting with water molecules and, eventually, oxygen sites at the dendrimer/water interphase, where the rheological properties of water are modified. Indeed, at low temperature, the spectrum of copper ions in pure water was computed with the parameters listed in Table 1 which are significantly different from those of Signal 3. Conversely, at room temperature, Signal 3 is the same as the spectrum of Cu(II) in pure water. This indicates that the ions fast exchange between the dendrimer/water interphase and the bulk water solution. The proposed structure for CuO<sub>4</sub> coordination responsible of Signal 3 is sketched in Figure 3c.

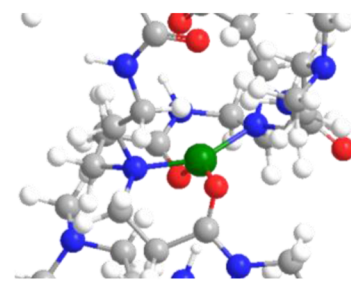
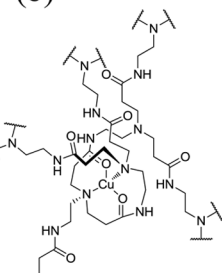
Therefore, the three signals, which progressively contribute to the EPR spectrum with the increase of Cu(II) concentration, indicate a progressive occupation of three different dendrimer regions: internal at the core for Signal 1 (Figure 3a), internal at the outer generations for Signal 2 (Figure 3b), and external at the dendrimer/water interface for Signal 3 (Figure 3c). Moreover, the three signals characterize both the interacting capability of the dendrimers toward the ions and, by means of the  $\tau$  parameter, the location of the ions in a more or less branch-crowded region and the flexibility of the dendrimer branches.

The EPR spectra (Figure 4, 150 K) at increasing Cu(II) concentrations in the presence of G5-Pyr showed the same three signals found for G3-Pyr. Signal 1 for G5-Pyr (Figure S2a, Supporting Information) was computed with the same

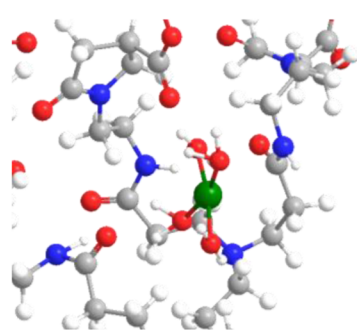
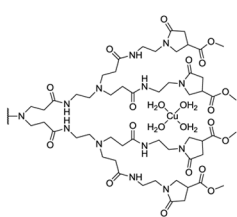
(a)



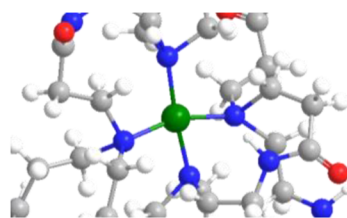
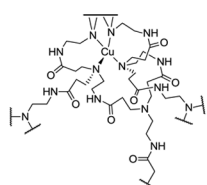
(b)



(c)



(d)



(e)

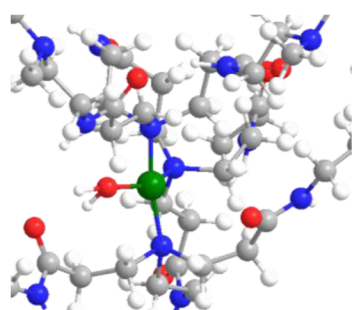
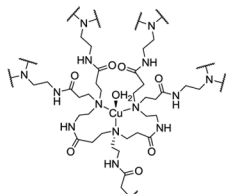


**Figure 3.** (a) CuN<sub>4</sub> coordination at the core; (b) CuN<sub>2</sub>O<sub>2</sub> coordination; (c) CuO<sub>4</sub> coordination; (d) CuN<sub>4</sub> coordination into the dendron structure; (e) CuN<sub>3</sub>O coordination for G4-Pyr.

magnetic parameters used for computing Signal 1 for G3-Pyr (Table 1).

At room temperature, the signals line shapes were almost the same for G3-Pyr and G5-Pyr. At low temperature, the spectra of G5-Pyr at the Cu(II) concentrations of 0.01 and 0.025 M revealed interesting differences (simulations shown in Figures S2a and S2b, respectively, in the Supporting Information; magnetic parameters in Table 1). At the lower Cu(II) concentration (0.01 M), the signal becomes less anisotropic in the  $A_{xx}$  and  $A_{yy}$  components, and the line width decreases with respect to 0.025 M, where Signal 1 for G5-Pyr is identical to Signal 1 for G3-Pyr. The lower anisotropy indicates a more organized and symmetric internal structure of G5-Pyr at [Cu(II)] = 0.01 M with respect to G3-Pyr at the same copper concentration. The lower line width for G5-Pyr is due to the larger availability of nitrogen internal sites for this dendrimer with respect to G3-Pyr. The complexed ions in the G5-Pyr dendrimer do not magnetically affect each other (negligible spin–spin interactions) at [Cu(II)] = 0.01 M since they do not occupy neighboring dendrimer cavities. Therefore, we may

hypothesize a different structure of the Cu(II) complexes into the G5-dendrimer cavities, as sketched in Figure 3d, which is in line with the coordination proposed by Diallo et al.<sup>45</sup> for other PAMAM dendrimers.

The main difference between the EPR spectra of G3-Pyr and G5-Pyr resides in the different variations of the relative percentages of the three signals as a function of Cu<sup>2+</sup> concentration (at constant dendrimer concentration in Pyr groups = 0.1 M), shown in Figure 5 for G3-Pyr (a) and G5-Pyr (b), respectively.

As we see in Figure 5, the three different Signals contribute to the EPR spectra in different Cu concentration ranges related to their “appearance” and eventual “disappearance”. For instance, it can be seen that Signal 1 started decreasing in relative percentage at Cu(II) concentrations higher than 0.1 M for G3-Pyr, while, for G5-Pyr, this reduction started at a Cu(II) concentration of 0.01 M. Indeed, at Cu(II) concentration of 0.01 M a small amount (28%) of Signal 2 contributed to the EPR spectrum. Besides, Signal 2 contributed to a very small Cu(II) concentration range for G5-Pyr with respect to G3-Pyr,

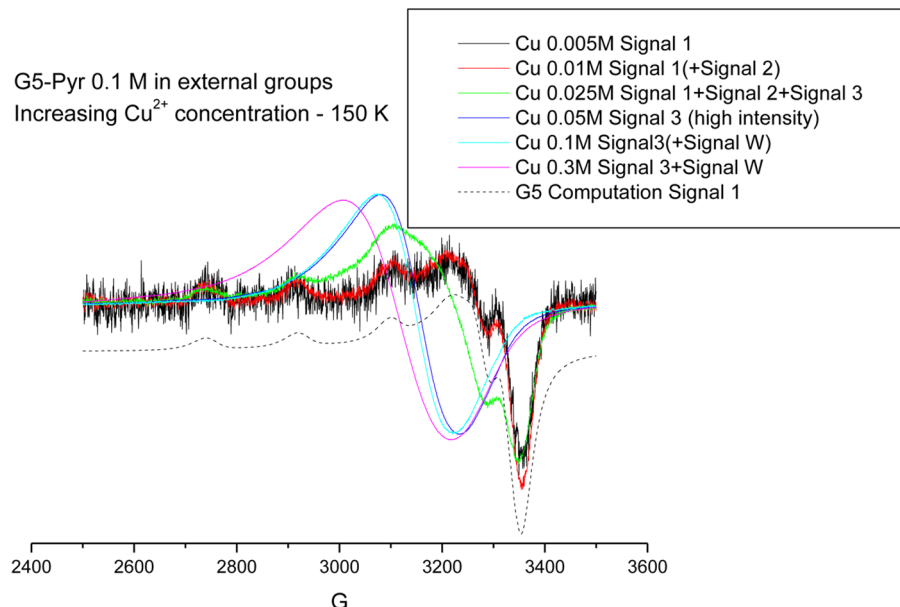


Figure 4. EPR experimental spectra at 150 K and at increasing Cu(II) concentrations in the presence of G5-Pyr 0.1 M.

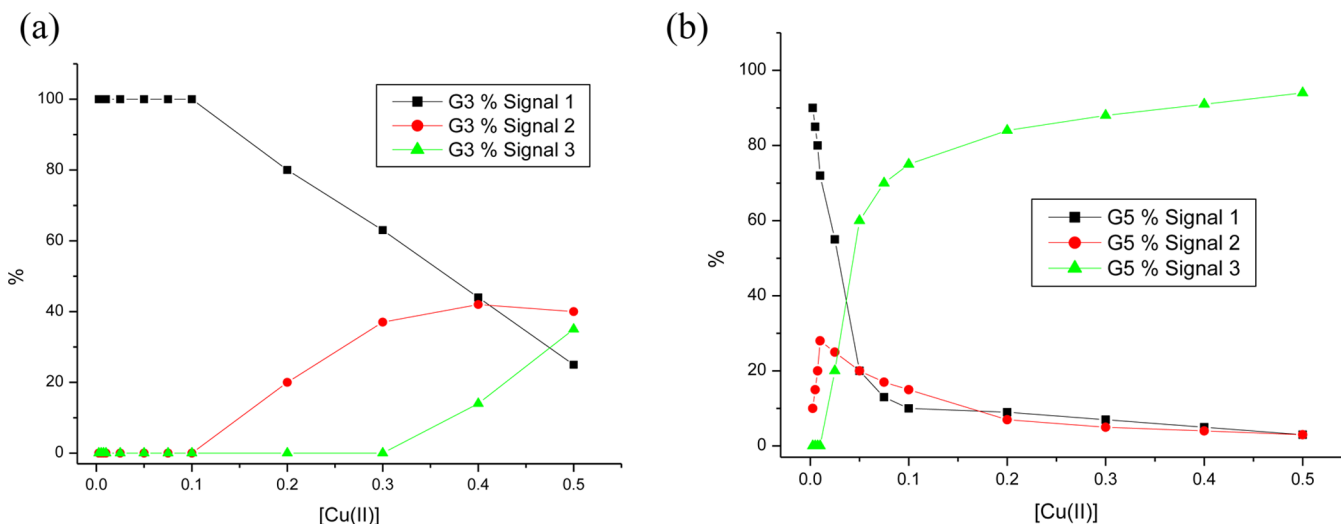


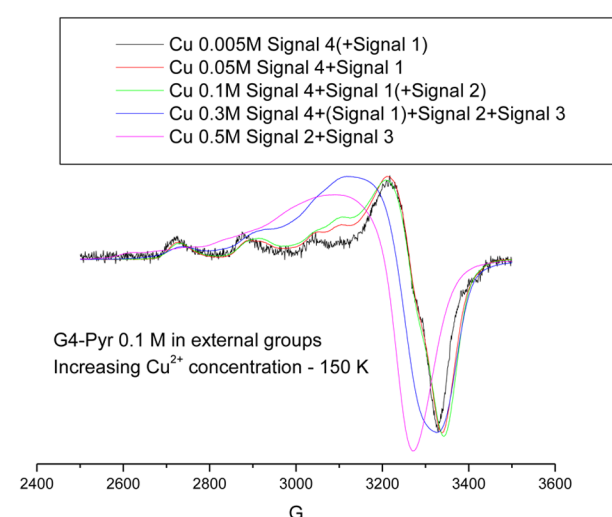
Figure 5. Variations of the relative percentages of Signals 1, 2, and 3 as a function of Cu(II) concentration for G3-Pyr (a), and G5-Pyr (b) at constant dendrimer concentration in Pyr groups (0.1 M).

because Signal 3 already started contributing (20%) at [Cu(II)] = 0.025 M for G5-Pyr. The reason for this “early” disappearance of Signal 1 and appearance of Signals 2 and 3 is mainly due to the involvement of the core in the coordination and it acts as proof of the CuN<sub>4</sub> structure proposed in Figure 3a. To better explain this point, it has to be remembered that the dendrimer concentration is in external surface groups and 0.1 M corresponds to about 3 mM for G3-Pyr macromolecules and 0.7 mM for G5-Pyr. However, the crowded external structure of G5-Pyr dendrimer also plays a role, mainly in decreasing the relative amount of the CuN<sub>2</sub>O<sub>2</sub> coordination. First, the ions cannot easily enter the internal dendrimer structure due to the “barrier” created by the external crowded branches of G5-Pyr. Furthermore, the ions cannot be easily hosted among the tangled branches of G5-Pyr because the interacting sites cannot coordinate the ions in a well-defined geometry. Also, ion–ion repulsion plays a role in the extrusion of copper ions outside the dendrimers.

In line with this description, while the intensity variation of G3-Pyr spectra is proportional to the Cu(II) concentration, the intensity of G5-Pyr spectra is slightly increasing with Cu(II) concentration up to 0.025 M, when both Signals 1 and 2 contribute to the spectra. At [Cu<sup>2+</sup>] ≥ 0.025 M, when Signal 3 starts appearing and the relative percentages of Signals 1 and 2 decrease, the overall EPR intensity becomes high, and at the highest concentrations, it increases proportionally to the Cu(II) concentration. This indicates that, when the ions are entering the dendrimer structure, mainly in the external branches, strong spin–spin interactions occur due to ions close to each other, and the intensity diminishes. Then, repulsion finally prevails and the ions are forced to remain outside the dendrimer giving rise to Signal 3, where no spin–spin interactions are possible due to the availability of free external space outside the dendrimer.

However, at the highest Cu(II) concentrations, we see that Signal 3, at both room and low temperatures, changes into the

(a)



(b)

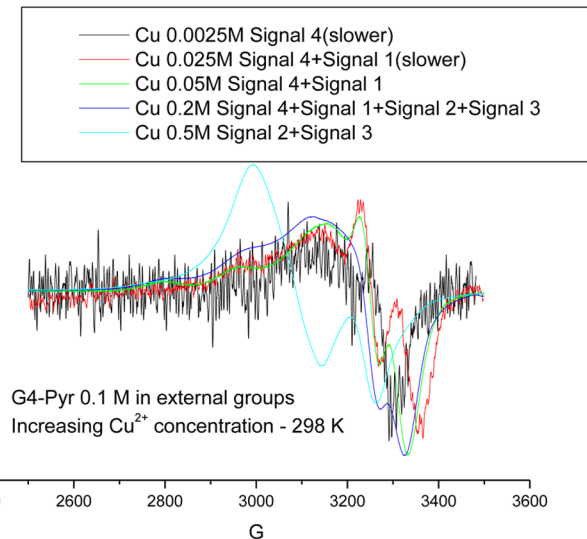


**Figure 6.** Selection of EPR experimental spectra of G4-Pyr dendrimer solutions by adding different Cu<sup>2+</sup> amounts, at 150 K (a) and 298 K (b).

kind of signal that is usually found for the ions in bulk water solution (Signal W), not affected by the dendrimer/water interphase. Therefore, the G5-Pyr/water interface saturates at relatively low Cu(II) concentration. We suppose that the high surface group density forces the ions to become fixed in close positions, and in order to avoid ion–ion repulsions, the ions move far away from the interphase, giving rise to Signal W.

As mentioned above, the results from G4-Pyr are discussed after the G3- and G5-Pyr, because G4-Pyr showed an unexpected behavior. We expected G4-Pyr to behave in between G3- and G5-Pyr. Conversely, G4-Pyr shows a higher degree of complexity when compared to G3- and G5-Pyr, as it is apparent from Figure 6, which displays selected spectra at 150 K (a) and 298 K (b) for the G4-Pyr dendrimer solution by adding different Cu<sup>2+</sup> amounts.

At the lowest copper concentrations (0.0025–0.005 M), the spectra of G4-Pyr solutions are constituted by a single component, which is different from the one obtained for the other generations. This component was termed Signal 4. The parameters for the simulations of the spectra listed in Table 1 (simulations shown in Figure S3a and S3b, Supporting Information, for Signal 4 at room and low temperature, respectively) indicate a CuN<sub>3</sub>O square planar distorted coordination. Therefore, differently from G3- and G5-Pyr, G4-Pyr does not show a CuN<sub>4</sub> coordination at the lowest Cu(II) concentrations. We suppose that the ions find a more “comfortable” location in the dendrimer interior coordinating three nitrogen and one oxygen sites with a different square planar geometry (sketched in Figure 3e), due to the constraint played by the pyrrolidone external units in the G4 dendrimer. However, this coordination confers more mobility ( $\tau = 0.85$  ns) to the G4-complexed ions with respect to the mobility ( $\tau = 1.67$  ns) of G3- and G5-complexed ions in the same experimental conditions (298 K).

At copper concentrations from 0.005 to 0.05 M, Signal 1 starts contributing and it increases in relative percentage at the expenses of Signal 4. Nevertheless, at 150 K, Signal 1 for G4-Pyr was the same as Signal 1 for G3-Pyr, and both Signals 1 and 4 remained unchanged in line shape, only changing their

relative percentages. On the contrary, at 298 K the situation is much more complicated, as described in the following:

- Signal 4 becomes progressively more mobile by increasing Cu(II) concentration. As an example, Figure S3c shows the simulation of the spectrum at [Cu<sup>2+</sup>] = 0.025 M, G4-Pyr 0.1 M, and T = 298 K. The parameters used for simulation are reported in Table 1. As we see, the simulation of Signal 4 at [Cu<sup>2+</sup>] = 0.025 M needed a  $\tau$  value of 0.3 ns that is about three times faster than  $\tau = 0.85$  ns needed at [Cu<sup>2+</sup>] = 0.0025 M. Therefore, at room temperature the progressive occupation of CuN<sub>4</sub> coordination sites into G4-Pyr allows the CuN<sub>3</sub>O complexes to gain freedom of motion.
- For Signal 1 at Cu(II) concentrations from 0.005 to 0.025 M (Figure S3c and Table 1), the G4-Pyr mobility at room temperature ( $\tau = 5.3$  ns) is slower than G3- or G5-Pyr mobility ( $\tau = 1.7$  ns). This means that, for G4-Pyr, the CuN<sub>4</sub> complex reported by Signal 1 is slowed down while the CuN<sub>3</sub>O complex reported by Signal 4 is sped up. In other words, the dendrimer branches forming the CuN<sub>4</sub> coordination show a lower mobility, while those involved in the CuN<sub>3</sub>O coordination show a higher mobility.
- Interestingly, another mobility transition occurs in between copper concentrations of 0.025 and 0.05 M (Figures S3c and S3d, respectively; parameters in Table 1): while Signal 4 does not change any more in mobility, Signal 1 finally comes back to the same mobility conditions ( $\tau = 1.7$  ns) found for G3-Pyr and G5-Pyr. This means that the mobility variations for the CuN<sub>4</sub> and CuN<sub>3</sub>O complexes are finally reaching an equilibrium condition where the relative percentage of CuN<sub>4</sub> becomes higher than that of CuN<sub>3</sub>O.

By adding a copper concentration higher than 0.05 M to G4-Pyr, first Signal 2, and then Signal 3 increase in intensity at the expenses of both Signal 4 and Signal 1. In detail, as better shown in Figure 7, we observe the following trends for the variation of the relative percentages of the four G4-Pyr signals as a function of Cu(II) concentration:

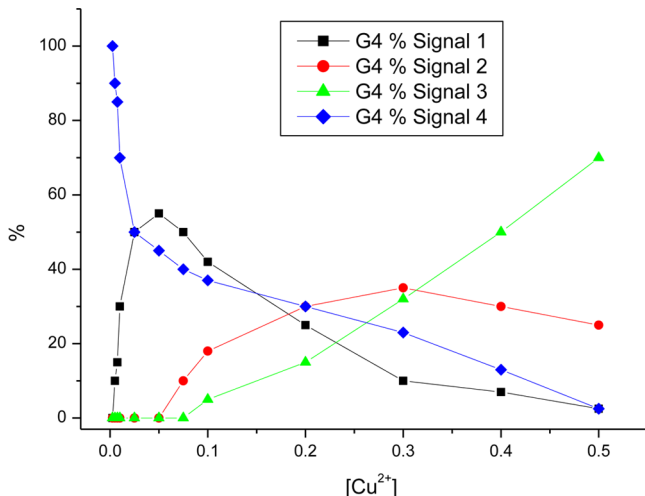


**Figure 7.** Variation of the relative percentages of the four Signals as a function of Cu concentration for G4-Pyr at constant dendrimer concentration in Pyr groups (0.1 M).

- At  $[Cu^{2+}] = 0.1$  M,  $CuN_4 \geq CuN_3O > CuN_2O_2 > CuO_4$ .
- At  $[Cu^{2+}] = 0.2$  M,  $CuN_3O = CuN_2O_2 \geq CuN_4 > CuO_4$ .
- At  $[Cu^{2+}] = 0.3$  M,  $CuN_2O_2 = CuO_4 \geq CuN_3O > CuN_4$ .
- At  $[Cu^{2+}] = 0.5$  M,  $CuO_4 > CuN_2O_2 > CuN_3O = CuN_4 \cong 0$ .

It is interesting to finally compare the graphs for the percentage variations in Figures 5 and 7 for the different generations, because, in spite of the unusual behavior of G4-Pyr, we may summarize some interesting common findings and trends, as follows:

- The higher the generation, the lower the Cu(II) concentration at which  $CuN_2O_2$  and  $CuO_4$  signals appear. In detail:
- The  $CuN_2O_2$  coordination starts contributing at 0.1 M for G3, 0.05 M for G4 and already at 0.005 M for G5.
- The  $CuO_4$  coordination starts contributing at 0.3 M, 0.075 and 0.025 M for G3-, G4-, and G5-Pyr, respectively. In the last case (G5-Pyr) the increase is very rapid, that is, in a very short copper concentration range.
- On the other hand, the higher the generation, the lower the copper concentration at which  $CuN_4$  coordination starts decreasing. In detail:
- Signal 1 starts decreasing at 0.1 M for G3-Pyr, 0.05 M for G4-Pyr and already at 0.005 M for G5-Pyr.
- The higher the generation, the “faster” (into a lower  $[Cu^{2+}]$  range) the decrease of  $CuN_4$  relative percentage.
- The higher the generation, the lower the Cu(II) concentration at which  $CuN_2O_2$  reaches a maximum relative amount.
- Finally, the higher the generation, the lower the maximum relative amount of  $CuN_2O_2$ .

In summary, by increasing generation, we need a lower Cu(II) amount to saturate the  $CuN_4$  coordination, which is in line with the involvement of the DAB core in this coordination, but also the  $CuN_2O_2$  coordination is much less contributing. The structure of G4-Pyr is “special” because it shows a different interacting ability and structural features with respect to the other PAMAM dendrimers, not only G4-Pyr at different generations, but also differently functionalized PAMAM dendrimers.<sup>8–10,45</sup>

## CONCLUSIONS

The EPR analysis of Cu(II) complexation by Gn-Pyr dendrimers at different generations (G3, G4, G5) allowed us to obtain a detailed view of the interacting ability of these dendrimers and useful information about their structure and flexibility. This information is precious for the purposes of using these dendrimers in biomedical fields. In this respect, G4-Pyr revealed a peculiar and unique behavior in its interacting modes, which may nicely justify the remarkably little toxicity in *in vitro* cell assays as well as very weak interactions with proteins. As a summary here, we want to underline the main peculiarities and differences of G4-Pyr if compared to other PAMAM dendrimers:

- The preferential coordination structure of G4-Pyr at low Cu<sup>2+</sup> concentrations is (distorted) square planar  $CuN_3O$ , where the oxygen site is very probably a water molecule. Moreover, this coordination permits fast mobility of the complexed ions. These results indicate an open-flexible structure at the core level, which is therefore able to host small guest molecules like drugs. In comparison to G4-Pyr in the same experimental conditions, G3-Pyr is able to form a  $CuN_4$  coordination as stable and slow moving complexes, similar to those identified for the other previously investigated PAMAM dendrimers.<sup>8–10,45</sup> G5-Pyr also shows a preferential  $CuN_4$  coordination which saturates at low Cu(II) concentrations, due to both saturation of core-nitrogen sites and to the constraint + barrier effect played by the external branches.
- Competition between the occupancy of  $CuN_3O$  and  $CuN_4$  coordination sites in the G4-Pyr mainly occurs in between 0.025 and 0.05 M of Cu<sup>2+</sup>. With respect to other PAMAM dendrimers,<sup>8–10</sup> the variation of the mobility of the Cu(II) complexes of G4-Pyr is peculiar. The  $CuN_4$  coordination shows a significantly slower rotational mobility at 298 K for G4-Pyr with respect to both G3- and G5-Pyr. This demonstrates that G4-Pyr has a good binding affinity toward Cu(II) ions.
- Further demonstration of the special binding ability of G4-Pyr is the contemporaneous persistence of the four different coordination modes,  $CuN_3O$ ,  $CuN_4$ ,  $CuN_2O_2$ , and  $CuO_4$  (at the water/dendrimer interface), in a large copper concentration range, up to 0.4 M, while no external coordination (with free water molecules) is recorded even at the highest Cu(II) amounts (above 0.5 M).

This study therefore provides useful pieces of information about the structure and interacting ability of Gn-Pyr dendrimers, which may be used as spin traps or for biomedical purposes.

## ASSOCIATED CONTENT

### Supporting Information

Simulations of EPR signals of Gn-Pyr+Cu(II) in different experimental conditions. This material is available free of charge via the Internet at <http://pubs.acs.org>.

## AUTHOR INFORMATION

### Corresponding Author

\*E-mail: maria.ottaviani@uniurb.it; jbc@chem.ku.dk.

### Notes

The authors declare no competing financial interest.

## ACKNOWLEDGMENTS

M.F.O. thanks PRIN2012 – NANOMed for financial support. COST Action MP1202 is also acknowledged.

## REFERENCES

- (1) Tomalia, D. A.; Christensen, J. B., Dendrimers as Nanomodules in the Nanotechnology Field: Designing Dendrimers. In *Designing Dendrimers*; Campagna, S., Ceroni, P., Puntoriero, F., Eds.; Wiley-VCH: Weinheim, DE, 2011; pp 1–33.
- (2) Tomalia, D. A. Dendrons/Dendrimers: Quantized, Nano-Element like Building Blocks for Soft-Soft and Soft-Hard Nano-Compound Synthesis. *Soft Matter* **2010**, *6*, 456–474.
- (3) *Dendrimers in Medicine and Biotechnology: New Molecular Tools*; Boas, U., Heegaard, P., Christensen, J. B., Eds.; Royal Society of Chemistry: Cambridge, U.K., 2006.
- (4) *Dendrimer-Based Nanomedicine*; Majoros, I., Baker, J. R., Jr., Eds.; Pan Stanford Publishing Pte. Ltd.: Singapore, 2008.
- (5) *Dendrimers, Dendrons, and Dendritic Polymers: Discovery, Applications, and the Future*; Tomalia, D. A., Christensen, J. B., Boas, U., Eds.; Cambridge University Press: Cambridge, 2012.
- (6) Ciolkowski, M.; Petersen, J. F.; Ficker, M.; Janaszewska, A.; Christensen, J. B.; Klajnert, B.; Bryszewska, M. Surface Modification of PAMAM Dendrimer Improves its Biocompatibility. *Nanomedicine* **2012**, *8*, 815–817.
- (7) Janaszewska, A.; Ciolkowski, M.; Wróbel, D.; Petersen, J. F.; Ficker, M.; Christensen, J. B.; Bryszewska, M.; Klajnert, B. Modified PAMAM Dendrimer with 4-Carbomethoxypyrrolidone Surface Groups Reveals Negligible Toxicity Against Three Rodent Cell Lines. *Nanomedicine* **2013**, *9*, 461–464.
- (8) Ottaviani, M. F.; Bossmann, S.; Turro, N. J.; Tomalia, D. A. Characterization of Starburst Dendrimers by the EPR Technique: 1. Copper Complexes in Water Solution. *J. Am. Chem. Soc.* **1994**, *116*, 661–671.
- (9) Ottaviani, M. F.; Montalti, F.; Turro, N. J.; Tomalia, D. A. Characterization of Starburst Dendrimers by the EPR Technique. Copper(II) Ions Full Generation Dendrimers. *J. Phys. Chem. B* **1997**, *101*, 158–166.
- (10) Ottaviani, M. F.; Valluzzi, R.; Balogh, L. Internal Structure of Silver-Poly(amidoamine) Dendrimer Complexes and Nanocomposites. *Macromolecules* **2002**, *35*, 5105–5115.
- (11) Appelhans, D.; Oertel, U.; Mazzeo, R.; Komber, H.; Hoffmann, J.; Weidner, S.; Brutschy, B.; Voit, B.; Ottaviani, M. F. Dense-Shell Glycodendrimers: UV/vis and Electron Paramagnetic Resonance Study of Metal Ion Complexation. *Proc. R. Soc. A* **2010**, *466*, 1489–1513.
- (12) Ottaviani, M. F.; Cossu, E.; Turro, N. J.; Tomalia, D. A. Characterization of Starburst Dendrimers by the EPR Technique: 2. Positively Charged Nitroxide Radicals of Variable Chain Length Used as Spin Probes. *J. Am. Chem. Soc.* **1995**, *117*, 4387–4398.
- (13) Ottaviani, M. F.; Turro, N. J.; Jockusch, S.; Tomalia, D. A. Characterization of Starburst Dendrimers by EPR. 3. Aggregational Process of a Positively Charged Nitroxide Surfactant. *J. Phys. Chem.* **1996**, *100*, 13675–13686.
- (14) Ottaviani, M. F.; Andechaga, P.; Turro, N. J.; Tomalia, D. A. Model for the Interactions between Anionic Dendrimers and Cationic Surfactants by means of the Spin Probe Method. *J. Phys. Chem.* **1997**, *101*, 6057–6065.
- (15) Ottaviani, M. F.; Matteini, P.; Brustolon, M.; Turro, N. J.; Jockusch, S.; Tomalia, D. A. Characterization of Starburst Dendrimers and Vesicle Solutions and Their Interactions by cw- and Pulsed-EPR, TEM, and Dynamic Light Scattering. *J. Phys. Chem.* **1998**, *102*, 6029–6039.
- (16) Ottaviani, M. F.; Daddi, R.; Brustolon, M.; Turro, N. J.; Tomalia, D. A. Structural Modifications of DMPC Vesicles upon Interaction with Poly(amidoamine) Dendrimers Studied by cw-Electron Paramagnetic Resonance and Electron Spin Echo Techniques. *Langmuir* **1999**, *15*, 1973–1980.
- (17) Ottaviani, M. F.; Furini, F.; Casini, A.; Turro, N. J.; Jockusch, S.; Tomalia, D. A.; Messori, L. Formation of Supramolecular Structures between DNA and Starburst Dendrimers Studied by EPR, CD, UV, and Melting Profiles. *Macromolecules* **2000**, *33*, 7842–7851.
- (18) Ottaviani, M. F.; Sacchi, B.; Turro, N. J.; Chen, W.; Jockusch, S.; Tomalia, D. A.; An, E. P. R. Study of the Interactions between Starburst Dendrimers and Polynucleotides. *Macromolecules* **1999**, *32*, 2275–2282.
- (19) Ottaviani, M. F.; Jockusch, S.; Turro, N. J.; Tomalia, D. A.; Barbon, A. Interactions of Dendrimers with Selected Amino Acids and Proteins Studied by Continuous Wave EPR and Fourier Transform EPR. *Langmuir* **2004**, *20*, 10238–10254.
- (20) Klajnert, B.; Cangiotti, M.; Calici, S.; Majoral, J.-P.; Caminade, A.-M.; Cladera, J.; Bryszewska, M.; Ottaviani, M. F. EPR Study of the Interactions between Dendrimers and Peptides Involved in Alzheimer's and Prion Diseases. *Macromol. Biosci.* **2007**, *7*, 1065–74.
- (21) Ottaviani, M. F.; Mazzeo, R.; Cangiotti, M.; Fiorani, L.; Majoral, J.-P.; Caminade, A.-M.; Pedziwiatr, E.; Bryszewska, M.; Klajnert, B. Time Evolution of the Aggregation Process of Peptides Involved in Neurodegenerative Diseases and Preventing Aggregation Effect of Phosphorus Dendrimers Studied by EPR. *Biomacromolecules* **2010**, *11*, 3014–3021.
- (22) Tomalia, D. A.; Huang, B.; Swanson, D. R.; Brothers, H. M.; Klimash, J. W. Structure Control Within Poly(amidoamine) Dendrimers: Size, Shape and Regio-Chemical Mimicry of Globular Proteins. *Tetrahedron* **2003**, *59*, 3799–3813.
- (23) Bennett, B.; Antholine, W. E.; D'souza, V. M.; Chen, G. J.; Ustinyuk, L.; Holz, R. C. Structurally Distinct Active Sites in the Copper(II)-Substituted Aminopeptidases from *Aeromonas proteolytica* and *Escherichia coli*. *J. Am. Chem. Soc.* **2002**, *124*, 13025–34.
- (24) Wang, D. M.; Hanson, G. R. A New Method for Simulating Randomly Oriented Powder Spectra in Magnetic Resonance: The Sydney Opera House (SOPHE) Method. *J. Magn. Reson. A* **1995**, *117*, 1–8.
- (25) Budil, D. E.; Lee, S.; Saxena, S.; Freed, J. H. Nonlinear-Least-Squares Analysis of Slow-Motion EPR Spectra in One and Two Dimensions Using a Modified Levenberg–Marquardt Algorithm. *J. Magn. Res. A* **1996**, *120*, 155–189.
- (26) Beinert, H., Structure and Function of Copper Proteins: Report, on the Fourth La Cura Conference Held at Villa Giulia, Manziana, Rome, Italy, 4–8 September 1979. *Coord. Chem. Rev.* **1980**, *33*, 55–85
- (27) Malmstrom, G.; Vanngard, T. Electron Spin Resonance of Copper Proteins and Some Model Complexes. *J. Mol. Biol.* **1960**, *2*, 118–124.
- (28) Aasa, R.; Petterson, R.; Vanngard, T. Electron Spin Resonance Line-Widths in Solutions of Copper and Silver Dithiocarbamates. *Nature* **1961**, *190*, 258–259.
- (29) Gillard, R. D.; Lancashire, R. J.; OBrien, P. Isomers of  $\alpha$ -Amino Acids with Copper(II). Part VI. Novel Equilibria at High pH in Copper(II): Amino-Acid Solutions. *Trans. Met. Chem.* **1980**, *5*, 340–345.
- (30) Gampp, H. Investigation of Complex Equilibria in Solution by EPR Spectroscopy. *Inorg. Chem.* **1984**, *23*, 1553–1557.
- (31) McBride, M. Electron Spin Resonance Study of Copper Ion Complexation by Glyphosate and Related Ligands. *Soil Sci. Soc. Am. J.* **1991**, *55*, 979–985.
- (32) Hassanien, M. M.; Gabr, I. M.; Abdel-Rhman, M. H.; El-Asmy, A. A. Synthesis and Structural Investigation of Mono- and Polynuclear Copper Complexes of 4-Ethyl-1-(pyridin-2-yl) thiosemicarbazide. *Spectrochim. Acta* **2008**, *71(A)*, 73–79.
- (33) Yokoi, N.; Ueno, T.; Unno, M.; Matsui, T.; Ikeda-Saito, M.; Watanabe, Y. Ligand Design for the Improvement of Stability of Metal Complex Protein Hybrids. *Chem. Commun.* **2008**, 229–31.
- (34) Kozlevcar, B.; Segedin, P. Structural Analysis of a Series of Copper(II) Coordination Compounds and Correlation with their Magnetic Properties. *Croat. Chem. Acta* **2008**, *81*, 369–379.
- (35) Basosi, R.; Della Lunga, G.; Pogni, R. Copper Biomolecules in Solution. *Biol. Magn. Reson.* **2005**, *23*, 385–416.

- (36) Saladino, A. C.; Larsen, S. C. DFT Calculations of EPR Parameters of Transition Metal Complexes: Implications for Catalysis. *Catal. Today* **2005**, *105*, 122–133.
- (37) Zhang, J.; Junk, M. J. N.; Luo, J.; Hinderberger, D.; Zhu, X. X. 1,2,3-Triazole-Containing Molecular Pockets Derived from Cholic Acid: The Influence of Structure on Host–Guest Coordination Properties. *Langmuir* **2010**, *26*, 13415–13421.
- (38) Peisach, J.; Blumberg, W. E. Structural Implications Derived from the Analysis of Electron Paramagnetic Resonance Spectra of Natural and Artificial Copper Proteins. *Arch. Biochem. Biophys.* **1974**, *165*, 691–708.
- (39) Addison, A. W. Spectroscopic and Redox Trends from Model Copper Complexes. In *Copper Coordination Chemistry: Biochemical and Inorganic Perspectives*; Karlin, K. D., Zubieta, J., Eds.; Adenine Press: Guilderland, NY, 1983; pp 109–115.
- (40) Wei, N.; Murthy, N. N.; Karlin, K. D. Chemistry of Pentacoordinate  $[LCuII-Cl]_n^+$  Complexes with Quinolyl Containing Tripodal Tetradentate Ligands. *Inorg. Chem.* **1994**, *33*, 6093–6100.
- (41) Malachowski, M. R.; Huynh, H. B.; Tomlinson, L. J.; Kelly, R. S.; Furbee, J. W., Jr. Comparative Study of the Catalytic Oxidation of Catechols by Copper(II) Complexes of Tripodal Ligands. *J. Chem. Soc., Dalton Trans.* **1995**, 31–36.
- (42) Solomon, E. I.; Hanson, M. A., Bioinorganic Spectroscopy. In *Inorganic Electronic Structure and Spectroscopy: Applications and Case Studies*; Solomon, E. I., Lever, A. B. P., Eds.; John Wiley & Sons: New York, 2006; Vol. II, pp 1–130.
- (43) Hathaway, B. J.; Tomlinson, A. A. G. Copper(II) Ammonia Complexes. *Coord. Chem. Rev.* **1970**, *5*, 1–43.
- (44) Garribba, E.; Micera, G.; Sanna, D.; Strinna-Erre, L. The Cu(II)-2,2'-bipyridine System Revisited. *Inorg. Chim. Acta* **2000**, *299*, 253–261.
- (45) Diallo, M. S.; Christie, S.; Swaminathan, P.; Balogh, L.; Shi, X.; Um, W.; Papelis, C.; Goddard, W. A., III; Johnson, J. H., Jr. Dendritic Chelating Agents. 1. Cu(II) Binding to Ethylene Diamine Core Poly(amidoamine) Dendrimers in Aqueous Solutions. *Langmuir* **2004**, *20*, 2640–2651.
- (46) Tomalia, D. A.; Swanson, D. R.; Huang, B. Heterocycle Functionalized Dendritic Polymers. World Patent WO 2004/069878, 19 August 2004